Green Chemistry

PAPER

View Article Online
View Journal | View Issue

Cite this: *Green Chem.*, 2025, **27**, 12378

Upcycling of poly(ethylene terephthalate) waste plastics to terephthalonitrile

Phuc T. T. Nguyen, [a,b] Jiong Cheng,[a,c] Junyu Mi [a] and Ning Yan *[a,b,c]

Received 28th May 2025,
Accepted 29th August 2025

DOI: 10.1039/d5gc02680f

rsc.li/greenchem

Chemical upcycling of plastic waste represents an emerging approach to generate value-added chemicals and mitigate environmental impacts. Despite the significant role of terephthalonitrile in the production of bioactive compounds and high-value materials, sustainable and efficient methods for its production from plastic waste remain underexplored. In this work, we present a tandem process for the transformation of poly(ethylene terephthalate) (PET) waste into terephthalonitrile under mild conditions (≤120 °C). The process involves PET ammonolysis with ethylene glycol and ammonia, followed by liquid-phase dehydration of terephthalamide using Pd catalysts *via* a water-transfer mechanism. The dehydration step achieves complete conversion of terephthalamide with up to 68% selectivity for the dinitrile and 32% for the mononitrile. Using electrospray ionization mass spectrometry, we identified Pd complexes, predominantly Pd dimers, as the catalytic species, regardless of the Pd precursor used. Application of the tandem system to commercial PET bottles and fibers resulted in terephthalonitrile yields of 39–51 mol% based on the PET feedstock, even in the presence of pigments and chlorine. Life cycle analysis indicated that this process reduces CO_2 emissions by at least 28% compared to conventional terephthalonitrile production from *p*-xylene. This work introduces a promising strategy for the upcycling of PET waste into organonitrogen compounds with high selectivity and low environmental impact.

Green foundation

1. This work introduces a non-petroleum-based, mild pathway for producing terephthalonitrile and presents a selective upcycling method for polyethylene terephthalate (PET) waste plastics into valuable organonitrogen compounds.
2. Utilizing Pd catalysts, the process converts up to 78% of amide groups to nitriles without generating undesired byproducts, significantly enhancing atom economy compared to previous gas-phase PET conversions that often resulted in cracking and coke formation. Operating at low temperatures (≤120 °C), the method is less energy-intensive, reduces safety concerns and lowers equipment costs. Life cycle analysis indicates at least a 28% reduction in carbon footprint compared to conventional terephthalonitrile production pathways.
3. The carbon footprint of this process is expected to decrease further with forthcoming advancements in green energy and low-carbon acetonitrile production.

Introduction

Waste plastics with over 350 million tons generated annually[1] have emerged as an abundant carbon resource for the production of fuels, chemicals, and materials. Plastic products are dominated by polyethylene (PE) and polypropylene (PP), which together account for approximately 45% of total production,[2] and have been converted into valuable chemicals such as liquid alkanes,[3–5] olefins,[6] arenes,[7–10] carbonyls,[11,12] sulfates,[13] nitriles,[14] and amines.[15] Upcycling plastics not only mitigates the environmental impacts of plastic pollution but also recovers economic value that is typically lost through landfilling or incineration.[16–20] It has been shown that utilizing plastics as alternative feedstocks for processes such as the conversion of polyolefins to hydrocarbons[21] or mixed plastic waste into methane[22] significantly reduces the carbon footprint compared to petroleum-based pathways.

Poly(ethylene terephthalate) (PET) is the fourth most produced plastic, accounting for 6.2% of global plastic production, and is the most abundant aromatic plastic,[2] primarily used in textiles and packaging. The majority of PET waste is recycled into lower-quality PET through mechanical recycling, although there has been increasing attention in chemical re-

[a]*Department of Chemical and Biomolecular Engineering, National University of Singapore, 4 Engineering Drive 4, 117585, Singapore. E-mail: ning.yan@nus.edu.sg*
[b]*Joint School of National University of Singapore and Tianjin University, Fuzhou 350207, Fujian, China*
[c]*Centre for Hydrogen Innovations, National University of Singapore, Singapore 117580, Singapore*

cycling of PET to virgin-like PET using technologies such as hydrolysis,[23–25] glycolysis,[26,27] and methanolysis.[28,29] Alternatively, PET can be upcycled into high-value products such as arenes,[30,31] terephthalamide,[32] *p*-phenylenediamine[33] and dimethyl cyclohexane-1,4-dicarboxylate.[34]

Nitriles represent an important class of organonitrogen compounds with broad applications in pharmaceuticals, pesticides, dyes and polymeric materials.[35] They also serve as versatile precursors for the synthesis of functional compounds such as amines, amides, N-heterocycles, carboxylic acids and esters.[36,37] Among them, terephthalonitrile is a key aromatic dinitrile with a market value of USD 1.2 billion in 2024.[38] It is widely used as an intermediate in the synthesis of bioactive compounds,[39] nitrogen-containing polymers,[40,41] flame retardants,[42] supercapacitors[43] and optoelectronics.[44–46] Terephthalonitrile is primarily produced from *p*-xylene through ammoxidation with ammonia as the nitrogen source,[47] catalyzed by metal oxides such as V_2O_5–Nb_2O_5/Al_2O_3[48] or V_2O_5–Sb_2O_3/Al_2O_3[49] at 400–500 °C (Fig. 1). Alternatively, *p*-xylene can be converted to terephthalonitrile *via* a nitrooxidation pathway, using nitric oxide NO as the nitrogen source and a Cr_2O_3-based catalyst at 440 °C.[50] However, these processes rely on fossil-based, non-renewable *p*-xylene as feedstock, while the high reaction temperature and the use of corrosive chemicals also raise safety concerns and increase equipment costs. Furthermore, the processes have substantial carbon footprints due to both the extraction of *p*-xylene and the energy required for heating and distillation. Therefore, it is desirable to develop more sustainable terephthalonitrile production pathways that utilize non-petroleum feedstocks, require lower energy input and release lower carbon emissions.

Recent studies have demonstrated the conversion of plastic waste into organonitrogen compounds, offering alternative pathways alongside those derived from petroleum-based and bio-based resources.[51,52] Notable examples include the transformation of polylactic acid into alanine,[53–56] poly(*p*-phenylene oxide) into substituted anilines,[57,58] polyurethane into aromatic amines,[59,60] and polystyrene into benzonitrile.[61,62] Given the structural similarity between PET monomer units and terephthalonitrile, pathways exist for the upcycling of PET into terephthalonitrile. Blackmon *et al.* reported a non-catalytic gas-phase dehydration of PET-derived terephthalamide to terephthalonitrile at 290–375 °C, achieving a low terephthalonitrile yield of 29%.[41] Fang's group reported the catalytic pyrolysis of PET under an NH_3 atmosphere over $Ca(OH)_2$/Al_2O_3[63] and γ-Al_2O_3,[64,65] obtaining 33–58% terephthalonitrile yields at 500–550 °C. The low carbon yield in the desired product was attributed to the formation of coke and by-products such as benzonitrile and aromatic hydrocarbons *via* cracking. Besides the low yields, these transformations share a similar issue with conventional production from *p*-xylene: operation at high temperature.

In this work, we aim to design an improved pathway for the conversion of PET waste into terephthalonitrile under milder conditions (Fig. 1). The process consists of two steps: PET ammonolysis and liquid-phase dehydration to terephthalonitrile. Since the former has been relatively well studied,[32,41,66–69] we focus on establishing the latter transformation using Pd catalysts *via* a water transfer mechanism.[70–72] This strategy was first reported by Maffioli *et al.*[70] in 2005, enabling water transfer with acetonitrile as an acceptor to achieve high conversion and selectivity toward the nitrile. Subsequent studies have explored the development of more efficient nitrile-based water acceptors,[73] novel Pd catalyst designs (*e.g.*, $Pd_3P_{0.95}$,[74] trinuclear palladium(II) complexes[75]), non-aqueous reaction conditions using Selectfluor[72] and expansion of substrate scope to unsaturated and alkyl amides.[76] Nevertheless, the specific conversion of terephthalamide to terephthalonitrile *via* a water transfer mechanism, as well as its potential application in plastic upcycling, has not yet been investigated. In our study, we explored the feasibility of this pathway, identified active Pd species and elucidated the critical role of water. Leveraging on these, we developed a tandem process consisting of PET ammonolysis followed by Pd-catalyzed dehydration of terephthalamide, and demonstrated its sustainability through a notably reduced carbon footprint.

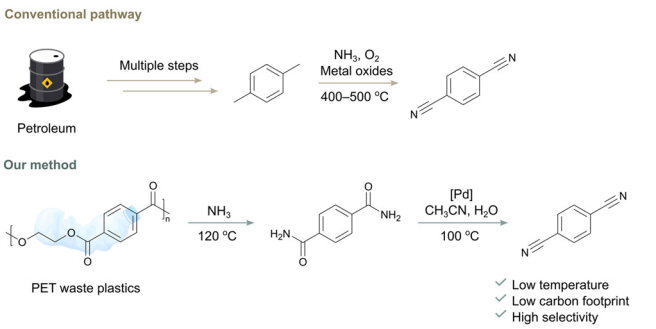

Fig. 1 Conventional pathway and our approach to terephthalonitrile.

Experimental

Materials

Terephthalamide (98%), 4-cyanobenzamide (98%) and terephthalonitrile (96.74%) were purchased from BLDPharm (China). PET (containing 30% glass fiber reinforcement), $PdCl_2$ (≥99.9%), $Pd(OAc)_2$ (≥99.9%), $Pd(NO_3)_2{\cdot}xH_2O$ (~40% Pd basis), palladium(II) acetylacetonate (99%), bis(acetonitrile) dichloropalladium(II) (99%), palladium(II) hexafluoroacetylacetonate, $Pd(OH)_2$/C (20 wt% Pd), Pd/C (10 wt% Pd), Pd/Al_2O_3 (10 wt% Pd), Pd/$BaSO_4$ (10 wt% Pd), bis(dibenzylideneacetone) palladium(0), tetrakis(triphenylphosphine)palladium(0) (99%) and Pd(0) EnCat® 30NP (0.4 mmol g^{-1} loading) were obtained from Sigma–Aldrich (Singapore). SiliaCat Pd(0) (0.24 mmol g^{-1} loading) and SiliaCat DPP-Pd (0.3 mmol g^{-1} loading) were purchased from Silicycle (Canada). Acetonitrile (≥99.5%) and ethyl acetate (≥99.5%) were obtained from VWR Chemicals (Singapore). PET fibers (3D × 64 mm) were purchased from Yizheng Zhicheng Chemical Fiber Co. Ltd (China).

$Pd(OH)_2$ was prepared by precipitation from a 0.045 M aqueous $Pd(NO_3)_2$ solution at pH 9 using a 0.1 M NaOH aqueous solution. The precipitate was collected by centrifugation, washed with water and dried at 60 °C overnight before use.

Reactions

The ammonolysis reaction of PET to terephthalamide was conducted in a 20 mL high-pressure autoclave equipped with a magnetic stirrer. Typically, PET (60 mg) and ethylene glycol (0.5 mL) were added to the autoclave, which was then sealed and purged with nitrogen at 5 bar for 10 cycles. The autoclave was subsequently purged with 3 bar NH_3 for 10 cycles and charged with 3 bar NH_3 at −20 °C for 15 minutes. The autoclave was then placed in a 120 °C steel holder and heated on a hotplate with stirring at 800 rpm for 7 h. Upon completion, the autoclave was cooled in an ice bath. The product mixture was vacuum-filtered through filter paper and washed with 20 mL of deionized water. The filter cake was dried at 60 °C overnight before being used for the dehydration reaction or further analysis.

The dehydration reaction of terephthalamide was conducted in a 15 mL cylindrical pressure vessel. Typically, terephthalamide (100 mg), $PdCl_2$ (6 mg), CH_3CN (3 mL) and H_2O (3 mL) were added to the vessel, which was then sealed. The mixture was magnetically stirred at 800 rpm and heated at 100 °C in an oil bath for 18 h. After the reaction, 5 mL of 2.5% aqueous NH_3 solution was added to convert the Pd species into inactive, water-soluble ammonia complexes. The resulting mixture was then extracted with ethyl acetate (3 mL × 3) and the organic phase was dried over Na_2SO_4. The products were quantitatively analyzed by gas chromatography with flame ionization detection (GC-FID) using dodecane as an internal standard (Fig. 2a).

For the reverse reaction (Fig. 3e), terephthalonitrile was used instead of terephthalamide under similar conditions. After the reaction, the mixture was filtered through filter paper. The solid was dried and weighed to determine the terephthalamide yield, while the filtrate was analyzed by GC-FID to determine the 4-cyanobenzamide yield and conversion.

For the quantification of acetamide (Table S1), the reaction mixture was treated with 30 mg of 2-mercaptobenzothiazole to precipitate Pd species, then filtered and analyzed by GC–FID using butan-1-ol as the internal standard. For the recycling test (Fig. 5c), the dehydration reaction was conducted with 50 mg terephthalamide for 6 h. Upon completion, solvents from the reaction mixture were completely evaporated at 60 °C using a rotary evaporator. The obtained solid was washed with 18 mL of water and filtered through filter paper. The filter cake containing terephthalonitrile was dissolved in ethyl acetate and quantified by GC-FID with dodecane as an internal standard. Meanwhile, the filtrate was evaporated at 140 °C using a rotary evaporator for 1 h to remove water and acetamide. The remaining solid containing 4-cyanobenzamide and the Pd catalyst was mixed with terephthalamide (25 mg), CH_3CN (3 mL) and water (3 mL) for the next recycling cycle.

Characterizations

Gas chromatography (GC) analysis was performed using an Agilent 7890A GC equipped with an HP-5 column and a flame ionization detector. The heating program involved ramping from 60 °C to 300 °C at 10 °C min^{-1}, followed by holding at 300 °C for 11 minutes. Nuclear magnetic resonance (NMR) spectroscopy was conducted using a Bruker Ascend 400 MHz spectrometer with D_2O or DMSO-d_6 as the solvent, and ethylene carbonate as an internal standard when required. Fourier-transform infrared (FT-IR) spectra were recorded on a Bruker VERTEX 70 with the range of 400–4000 cm^{-1}. Liquid samples for FT-IR were dropped onto the sample holder and evaporated at room temperature until the solvent signal disappeared, then measured in attenuated total reflectance (ATR) mode.

UV-visible (UV-Vis) measurements were performed using a Shimadzu UV-1900 UV-Vis spectrophotometer. Samples for UV-Vis measurements were prepared by dissolving Pd catalysts in the solvents at 0.1 mg mL^{-1}, sonicating for 10 minutes and filtering through 0.45 μm PES membrane filters. Electrospray ionization mass spectrometry (ESI-MS) was performed using an Agilent 6546 Q-TOF LCMS. The simulated MS spectra were generated using mMass. Inductively coupled plasma optical emission spectroscopy (ICP-OES) was performed on a Thermo Scientific iCAP 6000 series ICP spectrometer.

Life cycle analysis (LCA)

LCA was performed using the allocation, cut-off method. Data for CO_2 emissions were obtained from Ecoinvent 3.8 or the analysis by Cullen *et al.*[77] unless otherwise specified. Physical property data for the components were sourced from Aspen HYSYS and the NIST Chemistry WebBook unless stated otherwise. CO_2 emissions were considered from two main sources: materials and energy consumption. For comparison, the CO_2 emissions from the production of terephthalonitrile from *p*-xylene were calculated based on data reported by Golden *et al.*[49]

Results and discussion

Condition screening for the conversion of terephthalamide to terephthalonitrile

Since Pd catalysts are known for their activity in the water transfer mechanism between acetonitrile and monoamides,[70–72] we screened various homogeneous and heterogeneous Pd catalysts for the dehydration of terephthalamide (Fig. 2b). Pd salts, including $PdCl_2$, $Pd(NO_3)_2{\cdot}2H_2O$ and $Pd(OAc)_2$, as well as complexes such as $Pd(CH_3CN)_2Cl_2$ and $Pd(hfac)_2$ yielded high conversions (86–100%) and high terephthalonitrile yields with up to 56% when $PdCl_2$ was employed. Meanwhile, Pd coordinated with strong ligands such as $Pd(PPh_3)_4$ and $Pd(dba)_2$ and supported Pd catalysts showed low activity. Using acetonitrile as co-solvent, water demonstrated unique activity in this transformation, while other polar aprotic solvents showed trace or no activity (Fig. 2c). DMSO, the only tested solvent that can dissolve terephthalamide at room temperature, was employed but failed to produce nitrile products.

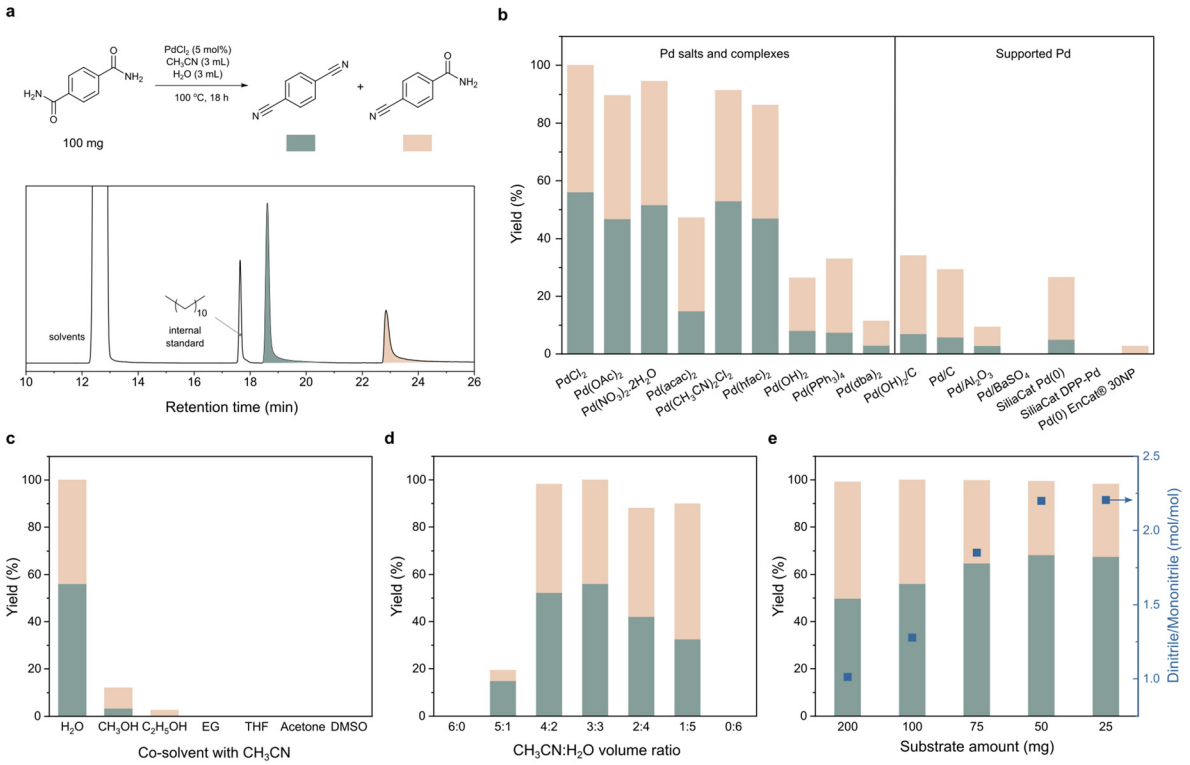

Fig. 2 (a) GC spectrum of the reaction starting from terephthalamide. Effect of (b) different Pd catalysts, (c) co-solvent with CH_3CN, (d) CH_3CN : H_2O volume ratio and (e) terephthalamide amount. Reaction conditions: terephthalamide (100 mg), $PdCl_2$ (5 mol%, 6 mg), CH_3CN (3 mL), H_2O (3 mL), 100 °C, 18 h. acac: acetylacetonate, hfac: hexafluoroacetylacetonate, dba: dibenzylideneacetone, EG: ethylene glycol, THF: tetrahydrofuran, DMSO: dimethyl sulfoxide.

We also found that the reaction is sensitive to the water-to-acetonitrile ratio. A volcanic-shaped trend was observed when the solvent ratio was changed, with the maximum yield obtained at a 1 : 1 ratio (Fig. 2d). When the substrate amount varied from 200 mg to 25 mg, we observed higher selectivity for terephthalonitrile over 4-cyanobenzamide, and the terephthalonitrile yield reached 68% (Fig. 2e). Further decreasing the $PdCl_2$ loading led to reduced terephthalonitrile yields, indicating that the catalyst amount should be maintained at 5 mol% as currently used (Fig. S1). At sufficient concentrations, $PdCl_2$ can fully convert terephthalamide to terephthalonitrile *via* the amide-to-nitrile pathway without detectable side reactions that introduce additional components into the system. The intermediate, 4-cyanobenzamide, can be transformed to terephthalonitrile with a 79% yield under the same conditions (Fig. S2). This represents an advantage over previous works,[63–65] where side reactions such as cracking, decarbonylation, alkylation, coupling, and oligomerization occurred during the conversion of PET to terephthalonitrile at high temperatures.

Kinetics and mechanisms of the water transfer reaction from terephthalamide to terephthalonitrile

To understand the reaction kinetics, the reaction was conducted at different temperatures for durations ranging from 1 h to 18 h (Fig. 3a–c). When the temperature increased from 80 °C to 120 °C, the terephthalonitrile yield rose from 54% to 61%. At 100 °C and 120 °C, the reaction reached equilibrium after 8 hours and 4 hours, respectively.

We then conducted NMR and FT-IR analyses to monitor the reaction progress over time. NMR spectra revealed the formation of acetamide and 4-cyanobenzamide in the reaction mixture at 100 °C (Fig. S3). Meanwhile, FT-IR showed a blue shift of 2–6 cm^{-1} in the absorption peaks of C═O, N–H, and C–N bonds[78] upon mixing terephthalamide with $PdCl_2$ (1 : 1 mass ratio) in CH_3CN/H_2O, suggesting interactions between Pd and the amide group (Fig. S4). The peak shifts of the C═O, N–H, and C–N bonds became more pronounced over time, which can be attributed to the transfer of the amide group from terephthalamide to acetonitrile.

Subsequently, we conducted control experiments starting from terephthalonitrile under similar reaction conditions (Fig. 3e). Without the Pd catalyst, almost no amide products were detected. In the presence of $PdCl_2$, around 20% of 4-cyanobenzamide was obtained, primarily through the hydrolysis of terephthalonitrile. This suggests that $PdCl_2$ can activate the nitrile group to facilitate hydrolysis.[79] When acetamide, the hydrolysis product of acetonitrile, was added, the hydration of terephthalonitrile significantly increased. A white solid was clearly observed when 5 equivalents of acetamide were added,

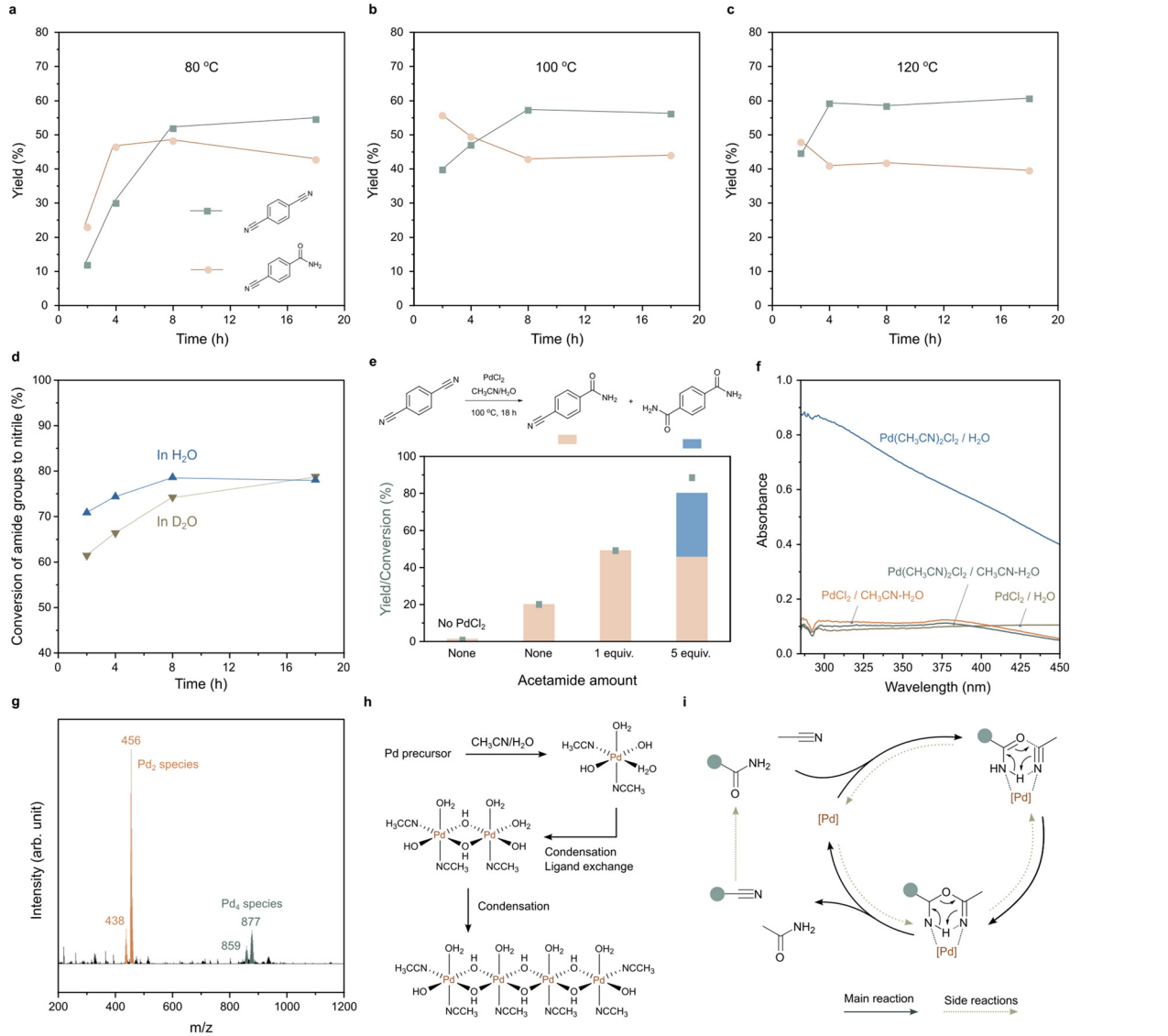

Fig. 3 Time–yield plots at (a) 80 °C, (b) 100 °C and (c) 120 °C. (d) Isotope effect. Reaction conditions: terephthalamide (100 mg), $PdCl_2$ (6 mg), CH_3CN (3 mL), H_2O or D_2O (3 mL). (e) Reversed reaction from terephthalonitrile. Reaction conditions: terephthalonitrile (100 mg), $PdCl_2$ (6 mg), CH_3CN (3 mL), H_2O (3 mL), acetamide (0–5 equivalent), 100 °C, 18 h. (f) UV-Vis spectra of Pd catalysts in H_2O and in the mixture of CH_3CN and H_2O (1 : 1 volume ratio). (g) ESI-MS spectra. Reaction conditions: terephthalamide (20 mg), $PdCl_2$ (6 mg), CH_3CN (3 mL), H_2O (3 mL), 100 °C, 2 h. Proposed (h) formation of active species and (i) reaction mechanism.

indicating the formation of terephthalamide. These findings confirm the existence of the Pd-catalyzed hydrolysis and the reverse water transfer from acetamide to the aromatic nitrile as side reactions. The reversible nature of the water transfer reaction also explains the decrease in terephthalonitrile selectivity when the feed concentration of terephthalamide increases, despite a sufficient reaction time (Fig. 2e).

We quantified the equilibrium concentration of acetamide by GC-FID for both the forward and reverse Pd-catalyzed water transfer reactions (Table S1). In the forward reaction from terephthalamide, the amount of acetamide formed was approximately equal to the amount of aromatic nitrile groups produced. In the reverse reaction from terephthalonitrile and acetamide, the decrease in acetamide corresponded closely to the amount of aromatic amide groups formed. These observations indicate that the Pd-catalyzed water transfer reaction is the dominant pathway, whereas hydrolysis of acetonitrile to acetamide is less significant. The equilibrium constant for the CH_3CN-mediated water transfer

$$\text{4-Cyanobenzamide} + CH_3CN \rightleftharpoons \text{terephthalonitrile} + CH_3CONH_2$$

is approximately 0.020, with nearly identical values obtained from both the forward and reverse reaction data.

Observing that not only $PdCl_2$ but also other Pd catalysts such as $Pd(NO_3)_2$ and $Pd(CH_3CN)_2Cl_2$ were active in the dehydration step, we hypothesized there may be common Pd active species for the reaction, regardless of the precursor used. Thus, we employed ESI-MS to identify the catalytic Pd species present in the reaction (Fig. 3g). The majority of Pd was detected as a dimeric complex (m/z = 456, Fig. S5c), together with its dehydrated form containing one fewer coordinated water molecule (m/z = 438). We also identified a tetrameric species (m/z = 877, Fig. S5d), likely formed through dimer condensation. These species were consistently observed when $Pd(NO_3)_2$ or $Pd(CH_3CN)_2Cl_2$ was used in place of $PdCl_2$, and even in the absence of terephthalamide (Fig. S5a). In contrast, when no $PdCl_2$ was added or when the catalytically inactive $Pd(dba)_2$ was used, these dimeric and tetrameric Pd complexes were not detected. When $Pd(NO_3)_2$ was used, a species containing one Pd atom was detected at m/z 329 (Fig. S5b). Furthermore, we collected the UV-Vis absorption spectra of $PdCl_2$ and $Pd(CH_3CN)_2Cl_2$ to compare their absorption patterns in H_2O and in CH_3CN/H_2O (Fig. 3f). Although their absorption patterns differ in H_2O, both $PdCl_2$ and $Pd(CH_3CN)_2Cl_2$ exhibit similar UV-Vis behavior in CH_3CN/H_2O, showing two characteristic peaks at 300 nm and 380 nm corresponding to Pd complexes.[80]

These findings confirmed our hypothesis on the formation of common catalytic Pd species regardless of the Pd precursor used, while for inactive Pd catalysts, they fail to form such species. It also highlights the critical role of both water and acetonitrile since these molecules remain in the coordination sphere of active Pd species. Plausibly, the Pd precursors are hydrolyzed and coordinated with CH_3CN and H_2O to form Pd $(CH_3CN)_x(H_2O)_y(OH)_t$ species, which subsequently condense into a dimer (major form) and a tetramer (minor form) (Fig. 3h). The presence of dehydrated forms of both the dimer and tetramer suggests dynamic behavior of the coordinated water molecules, which may either stabilize the complex through coordination to Pd or detach to generate vacant coordination sites for the substrates. When conducting the reaction in CH_3CN/D_2O, we observed a significantly lower reaction rate compared to that in CH_3CN/H_2O (Fig. 3d), further confirming the positive role of water.

A catalytic mechanism is proposed (Fig. 3i). The active Pd species coordinates with the nitrogen atoms of CH_3CN and the aromatic amide, facilitating the formation of a six-membered ring complex between the two components. Subsequently, a water molecule is transferred from the aromatic amide to CH_3CN. Since Pd can also activate the nitrile group in the product, the reverse reaction and hydrolysis can occur as side reactions. Nevertheless, these side reactions do not generate additional components within the reaction system. When testing the transformation of benzamides bearing different functional groups, we observed that the amide-to-nitrile conversion did not reach 100% (Fig. S2), further highlighting the reversible nature of the water transfer mechanism. Interestingly, benzamides with electron-withdrawing groups at the *para* position showed lower conversion. A possible explanation is that the electron-withdrawing effect decreases the electron density on the oxygen atom of the amide group, making bond formation between this oxygen and the nitrile group of acetonitrile more difficult. In the reaction, water not only coordinates with Pd to form the active species but also participates in proton exchange with amide groups, leading to a kinetic isotope effect when D_2O is used.

Tandem conversion of PET into terephthalonitrile

In the next step, we conducted the ammonolysis of PET in the presence of NH_3 and ethylene glycol (Table S2). Ethylene glycol served as the dispersion agent, heat transfer medium, and catalyst for PET ammonolysis.[67] This degradation process does not introduce additional organic components other than PET, ethylene glycol and terephthalamide into the system. After the reaction, terephthalamide was easily isolated as a white solid from the reaction mixture, which facilitates both separation and solvent recycling. The formation of terephthalamide at a 30% yield was observed when the reaction was conducted at 120 °C for 6 h (Table S2, entry 1). Employing $Zn(OAc)_2$ as a catalyst to facilitate ester bond cleavage[81] (Table S2, entry 2) did not improve the yield under these conditions. We hypothesized that the amount of ammonia was insufficient for effective ammonolysis and thus increased the ammonia/PET molar ratio by lowering the PET amount and feeding NH_3 at lower temperatures (Table S2, entries 3 and 4). This adjustment raised the terephthalamide yield up to 71% when ammonia was charged at −20 °C. The product exhibited high purity in the NMR spectrum in DMSO-d_6 with no by-products detected (Fig. 4a).

Attempts to develop a one-pot transformation from PET to terephthalonitrile by combining the ammonolysis and dehydration steps were unsuccessful, even when the dehydration step was performed in the presence of ammonia (Scheme S1). This incompatibility is likely due to the strong coordination between ammonia and $PdCl_2$, which deactivates the catalyst. Additionally, we found that residual ethylene glycol from the ammonolysis step negatively affected the dehydration step. This effect became pronounced when more than 5 equivalents of ethylene glycol were present, likely due to the formation of Pd black after the reaction (Fig. S6). Understanding the inhibitory effects of ethylene glycol and ammonia, we washed and dried the solid obtained from the ammonolysis step before subjecting it to the dehydration reaction. This procedure yielded terephthalonitrile at 27% yield along with 7% yield of 4-cyanobenzamide (Fig. 4b).

Recycling end-of-life PET to terephthalonitrile

We then applied our tandem reaction system to end-of-life PET items (Fig. 5a). After grinding, the PET samples underwent the same ammonolysis–dehydration tandem process as shown in Fig. 4b. The transparent PET bottle afforded a 51% yield of terephthalonitrile, while the green PET bottle gave a comparable yield of 49%. The green pigments were removed during the ammonolysis step (Scheme S2), producing white terephthalamide powder. Notably, this tandem process converted PET

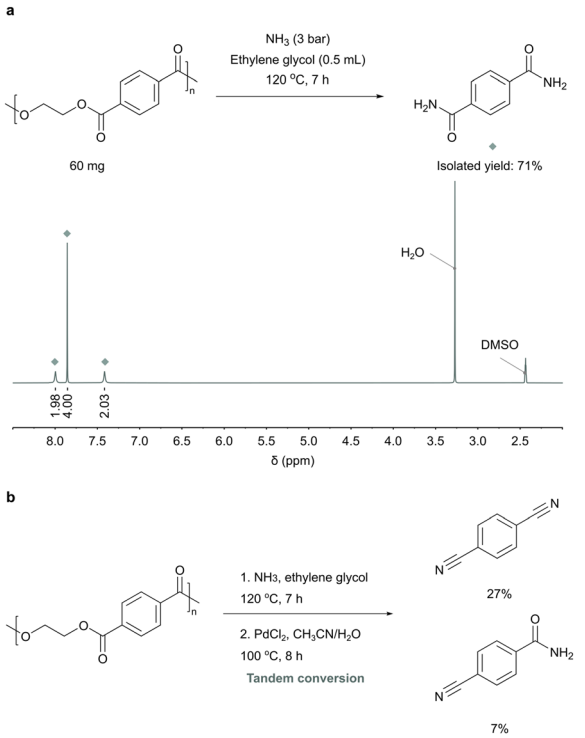

Fig. 4 (a) Ammonolysis of PET and the NMR spectrum of the product. (b) Tandem conversion of PET into terephthalonitrile. Reaction conditions for ammonolysis (step 1): PET (60 mg), ethylene glycol (0.5 mL), ammonia (3 bar, charged at −20 °C), 120 °C, 7 h. Reaction conditions for dehydration (step 2): product from step 1, $PdCl_2$ (6 mg), CH_3CN (3 mL), H_2O (3 mL), 100 °C, 8 h.

bottles to 45% terephthalonitrile even in the presence of 1 mass equivalent of polyvinyl chloride (PVC)—one of the most problematic contaminants in both mechanical and chemical recycling due to HCl release and chloride-induced poisoning of metal catalysts (*e.g.*, Ru, Pt).[82] Using PET fibers as the feedstock afforded a 39% yield of terephthalonitrile. Overall, these results highlight the system's capability to process commercial PET containers and textiles—the two largest applications of PET—while maintaining performance under challenging conditions such as pigments and chloride contamination.

Subsequently, we conducted recycling tests to evaluate the reusability of the $PdCl_2$ catalyst. An effective recyclability system should recover terephthalonitrile with high purity and remove acetamide, as its accumulation may promote the reverse reaction. To achieve this, we employed a workup method involving the evaporation of reaction solvents, followed by washing the resulting solid with water. Terephthalonitrile was isolated from the solid residue with high purity (terephthalonitrile to 4-cyanobenzamide molar ratio of 12.5 : 1, approximately 93% purity) (Fig. S7). The product was further purified by recrystallization from an acetonitrile–water mixture (1 : 1 volume ratio), yielding high-purity, long-needle crystals free of 4-cyanobenzamide (Fig. 5b). Meanwhile, most of the 4-cyanobenzamide, Pd catalyst, and acetamide remained in the water-soluble fraction. Using this approach, we isolated terephthalonitrile at 46% yield after the first cycle (Fig. 5c). The recovered 4-cyanobenzamide and Pd catalyst were mixed with fresh terephthalamide (at 50% of the amount used in the first cycle) for the subsequent runs. The accumulated yield of terephthalonitrile gradually declined over four cycles, primarily due to Pd catalyst loss as indicated by the fading yellow color after each cycle. ICP-OES revealed that 56% of the Pd content remained after the first reaction and workup cycle. The incomplete recovery of Pd is attributed to the oligomerization of Pd species, which form less water-soluble complexes and are therefore difficult to extract by water.

Nonetheless, this approach is superior to direct crystallization of terephthalonitrile after the reaction, which yields only 23% of terephthalonitrile in the first cycle and leads to incomplete conversion of terephthalamide in subsequent cycles (Fig. S8). This result demonstrates the viability of the recycling process, and future studies can focus on the oligomerization and/or immobilization of Pd species to minimize the catalyst loss.

Compared with previous studies on the upcycling of PET into terephthalonitrile, this work offers significant advantages: a low reaction temperature (≤120 °C) and high selectivity (Table S3). While other pathways yield oxygenates, coke, gases, and aromatics *via* side reactions, the Pd-catalyzed dehydration step enables high amide-to-nitrile selectivity with no other by-products detected. The intermediate, 4-cyanobenzamide, can be separated after the reaction by extracting with water (Fig. S7) and converted into terephthalonitrile with a 79% yield in one cycle (Fig. S2). However, as with all reported studies, catalyst reusability remains a limitation that should be addressed in future work.

Finally, we proposed a schematic diagram for the large-scale production of PET-derived terephthalonitrile (Fig. 5e) and performed an LCA to compare the carbon footprint of conventional terephthalonitrile production with that of our approach (Fig. S9 and Tables S4–S9). The proposed system comprises two jacketed reactors for ammonolysis and dehydration, two Nutsche filter-dryers for filtration, washing and drying, one evaporator for solvent recovery and one distillation unit for acetamide separation. This setup enables efficient recycling of solvents and unreacted substrates while producing two additional value-added compounds: ethylene glycol and acetamide.

Our analysis revealed that more than half of the total CO_2 emissions originate from solvent evaporation due to the high latent heat of water (Fig. S10), making the system highly sensitive to the feed concentration of terephthalamide in the dehydration step. Increasing the feed concentration from 8.3 kg m^{-3} (Scenario 3) to 33.3 kg m^{-3} (Scenario 1) resulted in a 2.7-fold reduction in CO_2 emissions from 22.8 kg CO_2 per kg terephthalonitrile to 8.5 kg CO_2 per kg terephthalonitrile despite a slight trade-off in product yield. Compared to the conventional approach from *p*-xylene, our approach achieves a 28% lower carbon footprint (Fig. 5d), benefiting from the utilization of end-of-life PET instead of fossil-based *p*-xylene, milder reaction conditions and the co-production of ethylene glycol and acetamide. From a green chemistry perspective, operating at a

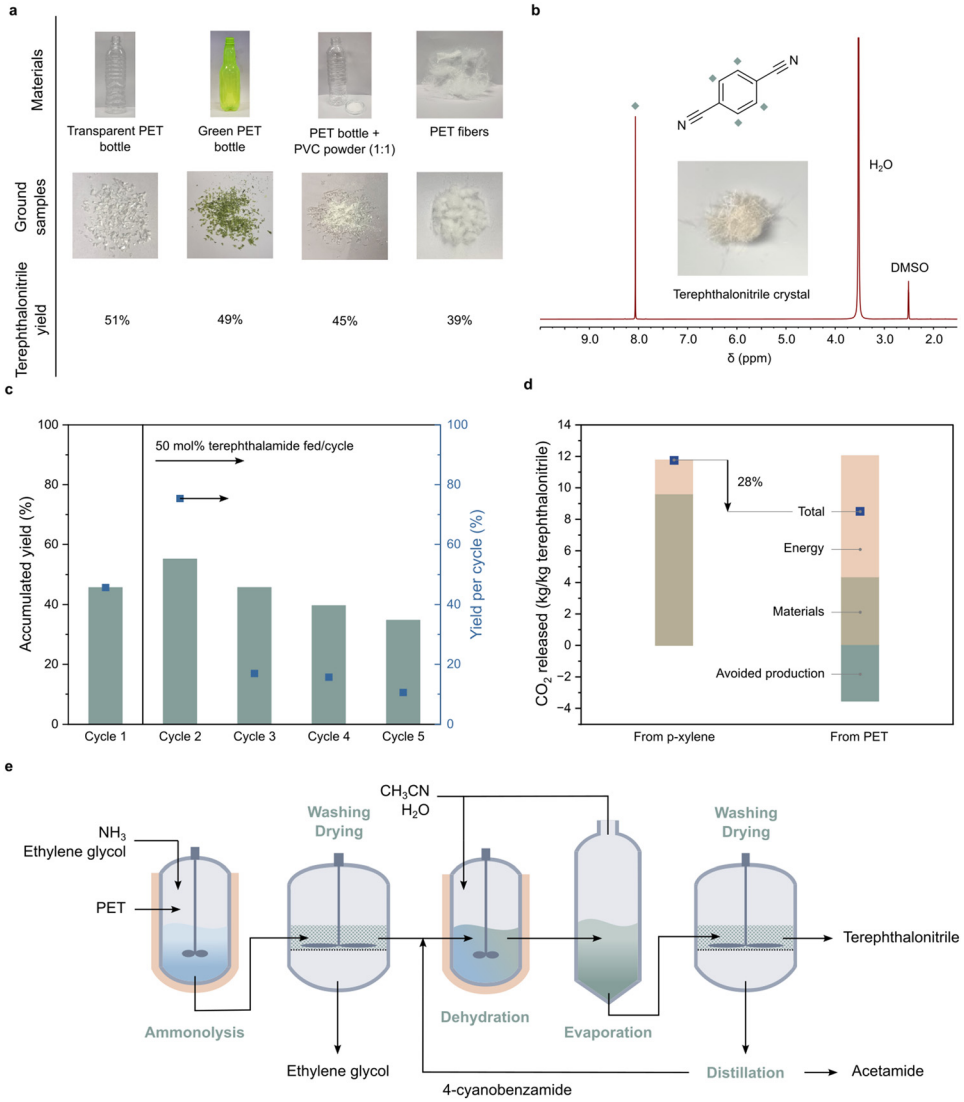

Fig. 5 (a) Tandem conversion of PET items into terephthalonitrile. In the case of the PET/PVC mixture, 1 : 1 refers to their mass ratio. Reaction conditions: same as in Fig. 4b. (b) NMR spectrum of terephthalonitrile crystallized after the reaction. Reaction conditions: terephthalamide (100 mg), $PdCl_2$ (6 mg), CH_3CN (3 mL), H_2O (3 mL), 100 °C, 8 h. (c) Recycing test. Reaction condition: terephthalamide (50 mg for the first cycle and 25 mg for the subsequent cycles), $PdCl_2$ (6 mg), CH_3CN (3 mL), H_2O (3 mL), 100 °C, 6 h. (d) Comparison of CO_2 released between the conventional approach and this work (Scenario 1 and Fig. S10). (e) Schematic diagram of the large-scale production of terephthalonitrile, ethylene glycol and acetamide from PET.

high feed concentration of 33.3 kg m^{-3} is expected to be more environmentally beneficial by reducing energy consumption and CO_2 emission. The main challenge at large scale lies in designing efficient product-separation and intermediate-recycling units, which can draw inspiration from industrial esterification processes with similar reversible nature.[83]

We further evaluated the impact of using low-carbon energy and feedstock sources (Fig. S11 and Table S10). Employing green ammonia, green acetonitrile and cleaner energy sources (hydrogen for heating and nuclear power for cooling) further reduced the CO_2 footprint to 2.0 kg CO_2 per kg terephthalonitrile (Scenario 4). In this scenario, the primary contributor to CO_2 emissions shifted from evaporation to acetonitrile production, accounting for over 60% of the total footprint. We anticipate that future advancements in the sustainable production of nitrogen-containing chemicals will further lower the CO_2 emissions associated with PET-based terephthalonitrile production.

Conclusions

In summary, we developed a tandem process to upcycle PET waste into terephthalonitrile under mild conditions. By combining PET ammonolysis with Pd-catalyzed dehydration *via* a water transfer mechanism, we achieved a high terephthalonitrile yield of up to 68% with no undesired by-products. Mechanistic investigations revealed the reversible nature of the

transformation, the critical role of water in the dehydration step and the formation of Pd dimeric complexes as the major catalytic species. Applying this process to end-of-life plastics demonstrated its feasibility in handling PET packaging and textile waste. The process is scalable using commercially available equipment, enabling the separation of high-purity terephthalonitrile alongside value-added ethylene glycol and acetamide. Moreover, life cycle analysis confirmed that our method offers 28% lower carbon footprint compared to conventional terephthalonitrile production, with further reductions achievable through the use of low-carbon feedstocks and clean energy sources. This study adds an example to integrate plastic upcycling with sustainable nitrogen chemical production, contributing to a circular carbon economy.

Author contributions

Phuc T. T. Nguyen: conceptualization, methodology, investigation, writing – original draft. Jiong Cheng: methodology. Junyu Mi: investigation. Ning Yan: supervision, writing – review & editing.

Conflicts of interest

There are no conflicts to declare.

Data availability

The data supporting this article have been included as part of the SI. Effect of catalyst amount, substituent groups, and residues from the ammonolysis step; equilibrium constant calculation; condition screening of the ammonolysis step; NMR spectra; FT-IR spectra; ESI-MS spectra; recycling test; conversion of green PET bottles; CO_2 emission calculations; comparison with previous works. See DOI: **https://doi.org/10.1039/d5gc02680f**.

Acknowledgements

N. Y. acknowledges the MOE Tier-2 project (MOE-T2EP10221-0020) from the Ministry of Education, Singapore and the National Research Foundation, Singapore, NRF Investigatorship (NRFI07–2021–0006) for the financial support. We thank Prof. Hai M. Duong (National University of Singapore) for providing the PET fibers, Dr Jinquan Chang for advice on ESI-MS analysis, and Ms Anh M. H. Trinh for assistance with some experiments.

References

1 OECD, Global Plastics Outlook,DOI: **10.1787/de747aef-en**, (accessed 1 August, 2024).
2 PlasticsEurope, Distribution of plastics production worldwide in 2023, by type [Graph]. In Statista., **https://www.statista.com/statistics/1559140/global-plastic-production-share-by-type/**, (accessed 12 August, 2025).
3 J. Yan, G. Li, Z. Lei, X. Yuan, J. Li, X. Wang, B. Wang, F. Tian, T. Hu, L. Huang, Y. Ding, X. Xi, F. Zhu, S. Zhang, J. Li, Y. Chen, R. Cao and X. Wang, *Nat. Commun.*, 2025, **16**, 2800.
4 W. Zhang, S. Kim, L. Wahl, R. Khare, L. Hale, J. Hu, D. M. Camaioni, O. Y. Gutiérrez, Y. Liu and J. A. Lercher, *Science*, 2023, **379**, 807–811.
5 C. Xing, C. Mao, S. Wang, Y. Zhou, L. Wu, D. Zhang, D. Kang, D. Yang, W. Gong, W. Wei, L. Wang, C. Li, G. A. Ozin, D. Yang and W. Sun, *Nat. Catal.*, 2025, **8**, 556–568.
6 J. Feng, J. Duan, C.-T. Hung, Z. Zhang, K. Li, Y. Ai, C. Yang, Y. Zhao, Z. Yu, Y. Zhang, L. Wang, D. Zhao and W. Li, *Angew. Chem., Int. Ed.*, 2024, **63**, e202405252.
7 Z. Chen, Z. Qiu, S. Lin and B. Lin, *Angew. Chem., Int. Ed.*, 2025, **64**, e202503355.
8 F. Zhang, M. Zeng, R. D. Yappert, J. Sun, Y.-H. Lee, A. M. LaPointe, B. Peters, M. M. Abu-Omar and S. L. Scott, *Science*, 2020, **370**, 437–441.
9 R. Gao, S. Mao, B. Lu, W. Liu and Y. Wang, *Angew. Chem., Int. Ed.*, 2025, **64**, e202424334.
10 Y. Ding, S. Zhang, C. Liu, Y. Shao, X. Pan and X. Bao, *Natl. Sci. Rev.*, 2024, **11**, nwae097.
11 Z. Xu, N. E. Munyaneza, Q. Zhang, M. Sun, C. Posada, P. Venturo, N. A. Rorrer, J. Miscall, B. G. Sumpter and G. Liu, *Science*, 2023, **381**, 666–671.
12 H. Li, J. Wu, Z. Jiang, J. Ma, V. M. Zavala, C. R. Landis, M. Mavrikakis and G. W. Huber, *Science*, 2023, **381**, 660–666.
13 N. E. Munyaneza, R. Ji, A. DiMarco, J. Miscall, L. Stanley, N. Rorrer, R. Qiao and G. Liu, *Nat. Sustain.*, 2024, **7**, 1681–1690.
14 B. Zhao, Z. Hu, Y. Sun, R. Hajiayi, T. Wang and N. Jiao, *J. Am. Chem. Soc.*, 2024, **146**, 28605–28611.
15 H. Li, A. A. Cuthbertson, A. A. Alamer, V. S. Cecon, H. Radhakrishnan, J. Wu, G. W. Curtzwiler, K. L. Vorst, X. Bai, C. R. Landis, G. T. Beckham and G. W. Huber, *Green Chem.*, 2024, **26**, 8718–8727.
16 S. Zhang, M. Li, Z. Zuo and Z. Niu, *Green Chem.*, 2023, **25**, 6949–6970.
17 C. Jehanno, J. W. Alty, M. Roosen, S. De Meester, A. P. Dove, E. Y. X. Chen, F. A. Leibfarth and H. Sardon, *Nature*, 2022, **603**, 803–814.
18 A. J. Martín, C. Mondelli, S. D. Jaydev and J. Pérez-Ramírez, *Chem*, 2021, **7**, 1487–1533.
19 A. C. Fernandes, *Green Chem.*, 2021, **23**, 7330–7360.
20 K. Ragaert, L. Delva and K. Van Geem, *Waste Manage.*, 2017, **69**, 24–58.
21 H. Ryou, J. Byun, J. Bae, D. K. Kim and J. Han, *Chem. Eng. J.*, 2025, **511**, 162256.
22 Z. Zhang, J. Wang, X. Ge, S. Wang, A. Li, R. Li, J. Shen, X. Liang, T. Gan, X. Han, X. Zheng, X. Duan, D. Wang,

J. Jiang and Y. Li, *J. Am. Chem. Soc.*, 2023, **145**, 22836–22844.
23 N. P. Murphy, S. H. Dempsey, J. S. DesVeaux, T. Uekert, A. C. Chang, S. Mailaram, M. Alherech, H. M. Alt, K. J. Ramirez, B. Norton-Baker, E. L. Bell, C. A. Singer, A. R. Pickford, J. E. McGeehan, M. J. Sobkowicz and G. T. Beckham, *Nat. Chem. Eng.*, 2025, **2**, 309–320.
24 S. Ügdüler, K. M. Van Geem, R. Denolf, M. Roosen, N. Mys, K. Ragaert and S. De Meester, *Green Chem.*, 2020, **22**, 5376–5394.
25 Y. Pang, X. Wu, Z. Li, J. Sun, Z. Li, J.-K. Qiu, J. Wang, C. Ma and K. Guo, *Green Chem.*, 2025, **27**, 6718–6724.
26 T. Yang, Q. Fan, H. He, C. Gao, Z. Yang and J. Xu, *Chem. Eng. J.*, 2025, **514**, 163038.
27 S. Shirazimoghaddam, I. Amin, J. A. Faria Albanese and N. R. Shiju, *ACS Eng. Au*, 2023, **3**, 37–44.
28 D. D. Pham and J. Cho, *Green Chem.*, 2021, **23**, 511–525.
29 S. Xie, C. Wang, W. Hu, J. Z. Hu, Y. Wang, Z. Dong, N. N. Intan, J. Pfaendtner and H. Lin, *Cell Rep. Phys. Sci.*, 2024, **5**, 102145.
30 M. Zhang, Z. Huo, L. Li, Y. Ji, T. Ding, G. Hou, S. Song and W. Dai, *ChemSusChem*, 2025, **18**, e202402013.
31 S. Hongkailers, Y. Jing, Y. Wang, N. Hinchiranan and N. Yan, *ChemSusChem*, 2021, **14**, 4330–4339.
32 J. Liang, J. Fu, H. Lin, J. Chen, S. Peng, Y. Sun, Y. Xu and S. Kang, *J. Ind. Eng. Chem.*, 2024, **132**, 578–587.
33 E. P. Neppel, R.-J. L. Peterson, L. Peereboom and J. R. Dorgan, *ACS Appl. Polym. Mater.*, 2025, **7**, 5475–5481.
34 Y. Li, M. Wang, X. Liu, C. Hu, D. Xiao and D. Ma, *Angew. Chem., Int. Ed.*, 2022, **61**, e202117205.
35 X. Wang, Y. Wang, X. Li, Z. Yu, C. Song and Y. Du, *RSC Med. Chem.*, 2021, **12**, 1650–1671.
36 H. Hu, S. Wu, F. Yan, M. Makha, Y. Sun, C.-X. Du and Y. Li, *J. Energy Chem.*, 2022, **70**, 542–575.
37 R. M. Rodrigues, D. A. Thadathil, K. Ponmudi, A. George and A. Varghese, *ChemistrySelect*, 2022, **7**, e202200081.
38 V. M. Reports, Global Terephthalonitrile Market Size By Application (Polymeric Materials, Dyes and Pigments), By End-Use Industry (Aerospace, Automotive), By Form (Solid, Liquid), By Grade (Industrial Grade, Pharmaceutical Grade), By Manufacturing Process (Liquid-phase Process, Gas-phase Process), By Geographic Scope And Forecast, **https://www.verifiedmarketreports.com/product/terephthalonitrile-market-size-and-forecast/**, (accessed 12 August, 2025).
39 W. P. Heilman, R. D. Battershell, W. J. Pyne, P. H. Goble, T. A. Magee and R. J. Matthews, *J. Med. Chem.*, 1978, **21**, 906–913.
40 G. Yu, J. Wang, C. Liu, E. Lin and X. Jian, *Polymer*, 2009, **50**, 1700–1708.
41 K. P. Blackmon, D. W. Fox and S. J. Shafer, *United States Pat*, US4973746A, 1990.
42 Y. Guo, Z. Chen, Y. Yu, T. Chen, Q. Zhang, C. Li and J. Jiang, *J. Appl. Polym. Sci.*, 2022, **139**, 52209.
43 L. Hao, B. Luo, X. Li, M. Jin, Y. Fang, Z. Tang, Y. Jia, M. Liang, A. Thomas, J. Yang and L. Zhi, *Energy Environ. Sci.*, 2012, **5**, 9747–9751.
44 G. V. Mageswari, Y. Chitose, Y. Tsuchiya, J.-H. Lin and C. Adachi, *Angew. Chem., Int. Ed.*, 2025, **64**, e202420417.
45 T. Raghava and S. Banerjee, *Chem. – Asian J.*, 2024, **19**, e202400898.
46 L. Morgan, G. Pavan, N. Demitri, C. Alberoni, T. Scattolin, M. Roverso, S. Bogialli and A. Aliprandi, *RSC Adv.*, 2023, **13**, 34520–34523.
47 P. Pollak, G. Romeder, F. Hagedorn and H.-P. Gelbke, in *Ullmann's Encyclopedia of Industrial Chemistry*, 2000, DOI: **10.1002/14356007.a17_363**.
48 R. D. Bushick and H. P. Angstadt, *United States Pat*, US3959337A, 1976.
49 R. L. Golden and H.-D. D. Yoo, *United States Pat*, US4419297A, 1970.
50 S. Zine, A. Sayari and A. Ghorbel, *Can. J. Chem. Eng.*, 1987, **65**, 127–131.
51 A. M. Afanasenko, N. Deak, J. October, R. Sole and K. Barta, *Green Chem.*, 2025, **27**, 5947–5981.
52 G. Liang, A. Wang, L. Li, G. Xu, N. Yan and T. Zhang, *Angew. Chem., Int. Ed.*, 2017, **56**, 3050–3054.
53 C. X. Liu, K. Liu, Y. Xu, Z. Wang, Y. Weng, F. Liu and Y. Chen, *Angew. Chem., Int. Ed.*, 2024, **63**, e202401255.
54 S. Tian, Y. Jiao, Z. Gao, Y. Xu, L. Fu, H. Fu, W. Zhou, C. Hu, G. Liu, M. Wang and D. Ma, *J. Am. Chem. Soc.*, 2021, **143**, 16358–16363.
55 Y. Wu, P. T. T. Nguyen, S. S. Wong, M. Feng, P. Han, B. Yao, Q. He, T. C. Sum, T. Zhang and N. Yan, *Nat. Commun.*, 2025, **16**, 846.
56 Y. Ma, X. Guo, M. Du, S. Kang, W. Dong, V. Nicolosi, Z. Cui, Y. Zhang and B. Qiu, *Green Chem.*, 2024, **26**, 3995–4004.
57 S. Jia, W. Zhao, X. Liu, Y. Guo and Y. Wang, *Sci. China: Chem.*, 2025, **68**, 520–525.
58 P. T. T. Nguyen, G. Gözaydın, J. Ma, B. Yao, Q. He and N. Yan, *Green Chem.*, 2024, **26**, 3949–3957.
59 V. Zubar, A. T. Haedler, M. Schütte, A. S. K. Hashmi and T. Schaub, *ChemSusChem*, 2022, **15**, e202101606.
60 L. Gausas, S. K. Kristensen, H. Sun, A. Ahrens, B. S. Donslund, A. T. Lindhardt and T. Skrydstrup, *JACS Au*, 2021, **1**, 517–524.
61 C. Sun, Y. Guo, X. Liu and Y. Wang, *Catal. Sci. Technol.*, 2025, **15**, 1905–1913.
62 G. Zeng, Y. Su, J. Jiang and Z. Huang, *J. Am. Chem. Soc.*, 2025, **147**, 2737–2746.
63 L. Xu, X.-w. Na, L.-y. Zhang, Q. Dong, G.-h. Dong, Y.-t. Wang and Z. Fang, *Catalysts*, 2019, **9**, 436.
64 G. Xie, G. Zhu, Y. Kang, M. Zhu, Q. Lu, C. He, L. Xu and Z. Fang, *J. Cleaner Prod.*, 2024, **434**, 140204.
65 L. Xu, L.-y. Zhang, H. Song, Q. Dong, G.-h. Dong, X. Kong and Z. Fang, *Waste Manage.*, 2019, **92**, 97–106.
66 P. Gupta and S. Bhandari, in *Recycling of Polyethylene Terephthalate Bottles*, ed. S. Thomas, A. Rane, K. Kanny, A. V. K. and M. and G. Thomas, William Andrew Publishing, 2019, pp. 109–134, DOI: **10.1016/B978-0-12-811361-5.00006-7**.

67 R.-J. L. Peterson, E. P. Neppel, L. Peereboom, P. A. Trinh, R. Y. Ofoli and J. R. Dorgan, *ACS Sustainable Chem. Eng.*, 2025, **13**, 4120–4131.
68 J. Huang, W. Xu, Y. Long, Y. Zhu, S. Chen, W. Duan, J. Ou, H. Wang, C. Dong and S. Tian, *Arabian J. Chem.*, 2024, **17**, 105719.
69 X. Luo, Q. Li and X. Chen, *Process Saf. Environ. Prot.*, 2025, **194**, 1584–1596.
70 S. I. Maffioli, E. Marzorati and A. Marazzi, *Org. Lett.*, 2005, **7**, 5237–5239.
71 H. Naka and A. Naraoka, *Tetrahedron Lett.*, 2020, **61**, 151557.
72 M. H. Al-Huniti, J. Rivera-Chávez, K. L. Colón, J. L. Stanley, J. E. Burdette, C. J. Pearce, N. H. Oberlies and M. P. Croatt, *Org. Lett.*, 2018, **20**, 6046–6050.
73 H. Okabe, A. Naraoka, T. Isogawa, S. Oishi and H. Naka, *Org. Lett.*, 2019, **21**, 4767–4770.
74 A. K. Sharma, H. Joshi, R. Bhaskar and A. K. Singh, *Dalton Trans.*, 2019, **48**, 10962–10970.
75 P. Dubey, S. Gupta and A. K. Singh, *Dalton Trans.*, 2017, **46**, 13065–13076.
76 W. Zhang, C. W. Haskins, Y. Yang and M. Dai, *Org. Biomol. Chem.*, 2014, **12**, 9109–9112.
77 L. Cullen, F. Meng, R. Lupton and J. M. Cullen, *Nat. Chem. Eng.*, 2024, **1**, 311–322.
78 A. Verma, R. K. Soni and M. Teotia, *J. Appl. Polym. Sci.*, 2019, **136**, 48022.
79 E. Tílvez, M. I. Menéndez and R. López, *Inorg. Chem.*, 2013, **52**, 7541–7549.
80 J. Bogojeski, J. Volbeda, M. Freytag, M. Tamm and Ž. D. Bugarčić, *Dalton Trans.*, 2015, **44**, 17346–17359.
81 W. Chen, M. Li, X. Gu, L. Jin, W. Chen and S. Chen, *Polym. Degrad. Stab.*, 2022, **206**, 110168.
82 P. A. Kots, B. C. Vance, C. M. Quinn, C. Wang and D. G. Vlachos, *Nat. Sustain.*, 2023, **6**, 1258–1267.
83 Z. Khan, F. Javed, Z. Shamair, A. Hafeez, T. Fazal, A. Aslam, W. B. Zimmerman and F. Rehman, *J. Ind. Eng. Chem.*, 2021, **103**, 80–101.